Engineered poplar for bioproduction of the triterpene squalene

Jacob D. Bibik[1,2,3], Abira Sahu[4,5], Boeun Kim[2,6], Faride Unda[2,7], Trine B. Andersen[2,3], Shawn D. Mansfield[2,7], Christos T. Maravelias[2,6,8], Thomas D. Sharkey[3,4,5], Björn R. Hamberger[1,2,3]

Affiliations

[1]Cell and Molecular Biology Program, Michigan State University, East Lansing, Michigan 48824, United States of America

[2]DOE Great Lakes Bioenergy Research Center, Michigan State University, East Lansing, Michigan 48824, United States of America

[3]Department of Biochemistry and Molecular Biology, Michigan State University, East Lansing, Michigan 48824, United States of America

[4]DOE Plant Research Laboratory, Michigan State University, East Lansing, Michigan 48824, United States of America

[5]The Plant Resilience Institute, Michigan State University, East Lansing, Michigan 48824, United States of America

[6]Andlinger Center for Energy and the Environment, Princeton University, Princeton, New Jersey 08544, United States

[7]Department of Wood Science, Faculty of Forestry, University of British Columbia, Vancouver, BC V6T 1Z4, Canada

[8]Department of Chemical and Biological Engineering, Princeton University, Princeton, New Jersey 08544, United States

ORCID numbers:

Jake Bibik: 0000-0002-8470-5459

Björn Hamberger: 0000-0003-1249-1807

Deleted: 3,

Commented [BH1]: Co-authors: Please check.

Commented [BH2]: Co-authors: Please add if you want it linked.

Abira Sahu: 0000-0001-9363-6929

Thomas D. Sharkey: 0000-0002-4423-3223

Email addresses: Sahu, Abira <sahuabir@msu.edu>; Boeun Kim <bk3460@princeton.edu>; Faride Unda <farideu@gmail.com>; Andersen, Trine <ande2202@msu.edu>; Mansfield, Shawn <shawn.mansfield@ubc.ca>; Christos Maravelias <maravelias@princeton.edu>; Sharkey, Thomas D. <TSHARKEY@MSU.EDU>.

Word count: 6,287

Abstract

Building sustainable platforms for production of biofuels and specialty chemicals has become an increasingly important strategy to supplement and replace fossil fuels and petrochemicals. Terpenoids are the most diverse class of natural products which have many commercial roles as specialty chemicals. Poplar is a rapidly growing, biomass dense bioenergy crop with many species known to produce large amounts of the hemiterpene isoprene, suggesting an inherent capacity to produce large amounts of other terpenes. Here we aimed to engineer poplar with optimized pathways to produce squalene, a triterpene commonly used in cosmetic oils, a potential biofuel candidate, and the precursor to the diverse classes of triterpenoids and sterols. The squalene production pathways were either re-targeted from the cytosol to plastids or co-produced with lipid droplets in the cytosol. Squalene and lipid droplet co-production appeared to be toxic, which we hypothesize to be due to disruption of adventitious root formation, suggesting a need for tissue specific production. Plastidial squalene production enabled up to 0.63 mg/g fresh weight in leaf tissue, which also resulted in reductions in isoprene emission and photosynthesis. These results were also studied through a technoeconomic analysis, providing further insight into developing poplar as a production host.

Key words

Squalene, plastid targeting, lipid droplet scaffolding, poplar NM6, photosynthesis, isoprene emission, technoeconomic analysis.

Introduction

Engineering plants for sustainable bioproduction of high-value chemicals has become of great interest (Yuan and Grotewold, 2015). One class of compounds of particular interest are terpenes and the further functionalized terpenoids, the most chemically diverse class of natural products. Terpenoid diversity throughout species has established their significance as major products in many herbal and medicinal plants used by humans for thousands of years (Pichersky and Raguso, 2018). Many plants are known for naturally producing large amounts of terpenes and terpenoids, including mono- and sesquiterpenoids in the Lamiaceae (mint) family, diterpenoid oleoresins in conifers, and isoprene in poplars (Bohlmann and Keeling, 2008). While these plants can produce these chemicals in relatively large amounts, scaling up for industrial production is often limited by a lack of plant biomass, accumulation of structurally similar compounds, low economic value, and many other factors. Furthermore, terpenoid diversity and complexity often makes them expensive and difficult, if not impossible, to chemically synthesize. With increased characterization of terpenoid biosynthesis in nature, biosynthetic pathways can be engineered into fast growing, non-food crop species as an inexpensive, ecologically sustainable, and larger scale alternative to chemical synthesis.

Terpenoids are derived from two common building blocks, dimethylallyl diphosphate (DMADP) and the isomer isopentenyl diphosphate (IDP), which are synthesized within plastids via the methylerythritol 4-phosphate (MEP) pathway or cytosolically from the mevalonate (MVA) pathway. The C_5 hemiterpenes, notably isoprene, are synthesized in plastids directly from one DMADP. The C_{10} monoterpenes and C_{20} diterpenes are also synthesized in plastids, using one DMADP and either one or three IDP molecules, respectively. Additionally, the C_{40} tetraterpenes (including carotenoids) are formed in plastids from two DMADP and six IDP molecules. Co-localized to the cytosol, or endoplasmic reticulum with access to cytosolic substrates, are the enzymes responsible for synthesis of the C_{15} sesquiterpenes and the C_{30} triterpenes. Many studies have developed strategies to engineer these pathways for increased production, re-direct biosynthesis between the cytosol and plastids, and even engineer co-production with, or scaffolding on lipid droplets (Wu *et al.*, 2006, 2012; Zhao *et al.*, 2018; Sadre *et al.*, 2019). Much of this research, however, has been performed using *Agrobacterium*-mediated transient expression. While recent efforts have made transient expression capable of producing terpenoids in gram-scale quantities (Reed *et al.*, 2017), there remains great interest in developing transgenic crops for economically and environmentally sustainable bioproduction. It is therefore important to translate these strategies from transient expression to stably transformed, transgenic lines in species capable of sustainable bioproduction.

Due to its rapid growth, high lignocellulosic biomass, and established production for the pulp and paper industry, many poplar (*Populus* spp.) hybrids have become target feedstocks for production of biofuels and bioproducts (Sannigrahi *et al.*, 2010). Bioengineering of poplar has been predominantly directed towards manipulation of the lignocellulosic content to improve conversion for pulp and paper, monolignol derived chemicals, or fermentable sugars (An *et al.*, 2021; Bhalla *et al.*, 2018; Zhou *et al.*, 2017). These fermentable sugars are then supplied as carbon sources for microbes, which in turn synthesize target biofuels and bioproducts, as opposed to the poplar directly producing the compounds. Recent analyses of another bioenergy feedstock crop, sorghum, have demonstrated potential to improve the economics of such systems by engineering the crops to directly produce higher-value chemicals, such as terpenes, which can be extracted prior to feedstock conversion (Yang *et al.*, 2020). These platforms would allow a more sustainable strategy for co-production of high-value chemicals and microbial feedstocks.

While most engineering of poplar has focused on production and conversion to monomeric sugars, there have been some examples of engineering for direct chemical production (Costa *et al.*, 2013; Lu *et al.*, 2017). One study engineered formation of the phenylalanine-derived 2-phenylethanol, and its phenylethanol glucoside form, which accumulated in leaves and stems of a poplar hybrid (Costa *et al.*, 2013). In an additional study, the same poplar hybrid was engineered with the pathways for either of the coniferyl alcohol derivatives eugenol or isoeugenol, which were further studied in 4-year field trials (Lu *et al.*, 2017). These biosynthetic pathways were targeted because they are derived from the same precursors of the monolignols that form lignocellulosic biomass in poplar. In addition to monolignol production, poplars are major contributors to global emissions of the hemiterpene isoprene, demonstrating significant metabolic capacity for production of terpenoids, particularly in leaves. Therefore, with poplars demonstrating robust growth and biomass production, ability to naturally produce large amounts of terpenes (isoprene), and having well-established deployment for industrial use, it is a promising platform for sustainable terpenoid production.

Squalene, C_{30} triterpene, is commonly used in cosmetic oils, vaccines, and is a candidate biofuel in addition to being the precursor to higher-value triterpenoids with broad biotechnological applications. Squalene biosynthesis in plants natively occurs through condensation of one DMADP and two IDP molecules to form farnesyl diphosphate (FDP) by the soluble FDP synthase (FDPS), followed by further condensation of two FDP molecules by the endoplasmic reticulum bound squalene synthase (SQS). The squalene production strategies were previously developed through transient expression to

successfully re-target FDPS and SQS to plastids or the surface of lipid droplets (Figure 1). We previously developed engineered squalene pathways to either re-target squalene biosynthesis from the cytosol to plastids or co-produce cytosolic lipid droplets with and without scaffolding of squalene biosynthetic enzymes at the surface (Bibik *et al.*, 2022). The first strategy used here in poplar engineering re-targets an *Arabidopsis thaliana* FDPS (*At*FDPS) and a SQS from the fungal species *Mortierella alpina* with a 17 amino acid C-terminal truncation to remove the endoplasmic reticulum retention sequence (*Ma*SQS CΔ17), to plastids by fusion with an N-terminal transit peptide from the *A. thaliana* Rubisco small subunit (Lee *et al.*, 2006) (Figure 1, right). To increase the amount of available IDP/DMADP in plastids, overexpression of the gene for 1-deoxy-D-xylulose-5-phosphate synthase from *Coleus forskohlii* (*Cf*DXS) was included. As the entry step to the MEP pathway, DXS has been shown to be rate limiting and overexpression of the gene can overcome some of these limitations.

Formatted: Small caps

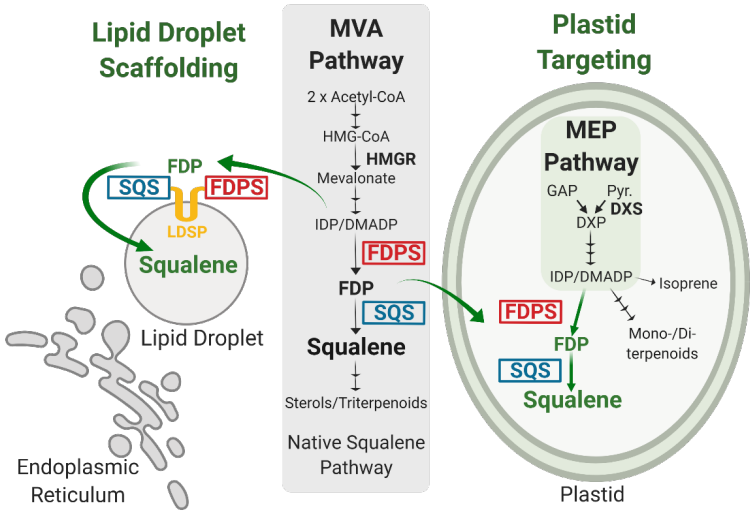

Figure 1: Representation of engineered squalene pathways used for poplar transformations. The enzymes required for biosynthesis of squalene, FDPS and SQS, were re-targeted to plastids (right) or used in combination with lipid droplet co-production or scaffolding through fusions with LDSP (left). These pathways utilize

Formatted: After: 0.81"

IDP/DMADP building blocks made available in plastids from the MEP pathway or in the cytosol from the MVA pathway. Variations of both strategies were attempted when engineering poplar.

The second strategy tested here was designed for co-production of cytosolic lipid droplets and squalene also utilizing *At*FDPS and *Ma*SQS CΔ17 (Figure 1, left). To upregulate production of IDP/DMADP in the cytosol, the gene encoding the committed step to the MVA pathway, 3-hydroxy-3-methylglutaryl-CoA reductase (HMGR), from *Euphorbia lathyris* (*El*HMGR$^{159\text{-}582}$) was included. Overexpression of the gene in truncated form of HMGR improves flux through the MVA pathway and increases cytosolic terpenoid yields (Sadre *et al.*, 2019). In addition to the squalene biosynthetic pathway, this strategy co-produces lipid droplets through expression of the gene for truncated WRINKLED1 transcription factor from *A. thaliana* (*At*WRI1$^{1\text{-}397}$), which upregulates expression of pathways involved with fatty acid and lipid production (Grimberg *et al.*, 2015; Ma *et al.*, 2015), as well as the gene for Lipid Droplet Surface Protein from *Nannochloropsis oceanica* (*No*LDSP), which inserts into and aids in formation of lipid droplets(Sadre *et al.*, 2019; Vieler *et al.*, 2012). Previous work has shown co-expressing *AtWRI1*$^{1\text{-}397}$ and *NoLDSP* with the soluble squalene pathway increased squalene yields in a *Nicotiana benthamiana* transient expression system, with even further increases when fusing *At*FDPS and *Ma*SQS CΔ17 to *No*LDSP, scaffolding the pathway on the surface of lipid droplets (Bibik *et al.*, 2022).

In this work, we aimed to engineer poplar for squalene production either through cytosolic lipid droplet scaffolding and co-production, which demonstrated the highest squalene yields in transient expression, or in plastids, which is where poplars natively produce isoprene (Figure 1). The hybrid poplar NM6 (*P. nigra* L. x *P. maximowiczii* A. Henry) is a female, clonally propagated, commercially valuable clone which has demonstrated rapid growth and biomass accumulation in northern climates (Labrecque and Teodorescu, 2005) and is amenable to engineering through *Agrobacterium*-mediated transformation (Yevtushenko and Misra, 2010; Ko *et al.*, 2012; Han *et al.*, 2013). We engineered poplar NM6 with overexpression constructs of squalene pathways, measured yields of transgenic lines throughout the crop, determined the effects of these pathways on photosynthesis and isoprene emission, and performed a technoeconomic analysis to gain insight into future production requirements. We also attempted to engineer the routinely manipulated poplar hybrid P39 (*P. alba* x *P. grandidentata*), though we were unable to generate transformants. While our efforts in poplar P39 were ultimately unsuccessful, engineering poplar NM6 to redirect terpenoid precursors away from isoprene

and towards terpenes and terpenoids of biotechnological interest may add value to poplar plantations, reduce greenhouse gas emission due to isoprene, and advance poplar as a bioproduct feedstock.

Results and Discussion

Engineering squalene production in transgenic NM6 poplar

To introduce these compartmentalized squalene pathways into hybrid poplar, two constructs for the plastid targeted squalene pathway, three constructs for the cytosolic lipid droplet pathways, and an empty vector were created for transformations (Figure 2). A modified pEAQ-*HT* vector (Peyret and Lomonossoff, 2013) containing two multiple cloning sites (MCS1 and MCS2) was used to generate construct variations for each transformation. The LP4/2A hybrid linkers (François *et al.*, 2004; Sun *et al.*, 2017), which enable co- and post- translational cleavage into separate protein products, were used to separate genes in a single MCS to allow expression of multiple genes from a single promoter (Figure 2). The two plastid targeting constructs were generated to contain either *CfDXS* and *AtFDPS* in MCS1, separated by LP4/2A, and *MaSQS CΔ17* in MCS2 (pDF1S2), or all three genes in MCS1, each separated by LP4/2A sequences, and an empty MCS2 (pDFS1E2). Three cytosolic lipid droplet constructs were created similarly but using *ElHMGR*$^{159\text{-}582}$ and *AtWRI1*$^{1\text{-}397}$ in addition to *AtFDPS* and *MaSQS CΔ17*, with variations in *No*LDSP fusion combinations (Figure 2). These three constructs were designed to enable co-production of lipid droplets and squalene with either soluble *At*FDP and *Ma*SQS CΔ17 (pWL1HFS2), soluble *At*FDPS and *Ma*SQS CΔ17 fused to *No*LDSP (pWSL1HF2), or both *At*FDPS and *Ma*SQS CΔ17 fused to *No*LDSP (pWH1SLF2).

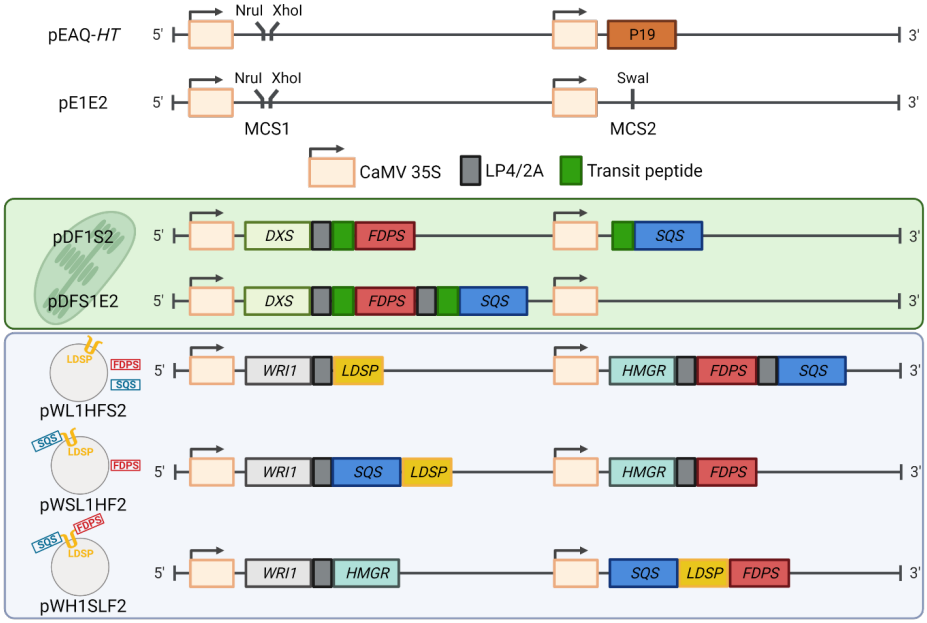

Figure 2: Construct design for squalene pathways used for poplar transformations. Constructs used in this study were derived from the pEAQ-*HT* vector (top) modified to contain two multiple cloning sites (MCSs). Constructs were designed for plastid targeting (green) or for lipid droplet co-production and scaffolding (grey) of the enzymes required for squalene biosynthesis.

Successful transformation of NM6 was initially only achieved with the empty vector construct, pE1E2 ("E" lines), and one of the constructs for plastid targeted squalene production, pDF1S2 ("F" lines). During regeneration of transformed poplar NM6, it was difficult to obtain transformants with pWL1HFS2. In some instances, shoots were formed from callus tissue, but upon transfer to rooting medium plantlets did not survive. To determine whether this was unique to NM6, this construct along with two other constructs with variations of squalene pathway lipid droplet scaffolding (Figure 2), were used in attempts to transform the hybrid poplar P39. Poplar P39 is a hybrid line suitable to lab manipulation and is commonly used for generating transformants. When transforming poplar P39, however, similar effects were observed for all three lipid droplet constructs where plantlets became chlorotic on rooting medium and did not survive, whereas transformed plantlets were able to be generated with the empty vector pE1E2. Further transformation attempts of poplar NM6 eventually led

Deleted: o

Deleted: o

to generation of transgenic plantlets with pWL1HFS2 (“G” lines), which were also included for analysis to determine if they could produce squalene at higher levels than empty vector lines.

A general analysis of squalene production was performed on leaf tissue across transformants and micro-propagated clones (Figure 3). One transformant with the pDF1S2 construct, F4-1, produced the highest squalene yield and the clones, F4-2 and F4-3, produced the second highest yields (Figure 3a). The two independent lines transformed with pWL1HFS2, G1 and G71, produced detectable levels of squalene, but not more significantly than the empty vectors (Figure 3b). Similar mean squalene yields were seen as before (Figure 4a) and, in general, higher yields were seen in older leaves (Figure 4b). The highest mean yield across leaf stages was 0.63 mg/g fresh weight (mg/gFW) as produced in line F4-1, with the highest mean yield in the seventh leaves at 0.89 mg/gFW. Variation is seen between micro-propagated clones when comparing squalene yields, especially in F4 lines. Studies have indicated significant changes in DNA methylation levels between early generations of micro-propagated clones (Vining *et al.*, 2013; Zhang *et al.*, 2021), which may be one explanation of the phenotypic variation but would require further investigation.

Deleted: s

Deleted: next

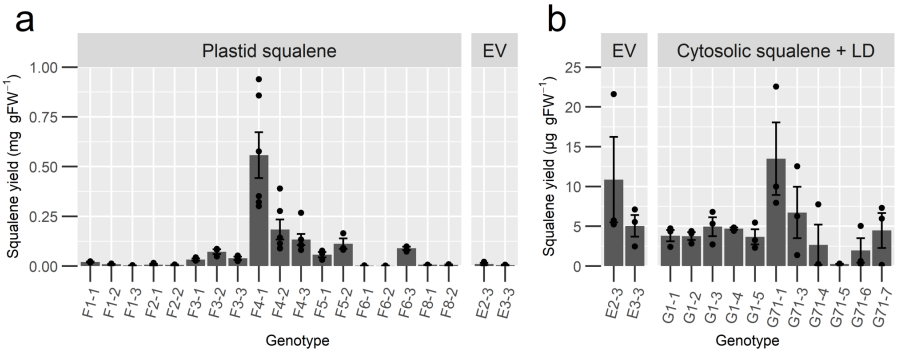

Figure 3: Survey of transgenic poplar for production of squalene in leaf tissue. Panel (a) shows poplar lines transformed with the plastid targeted squalene pathway in vector pDF1S2 compared with empty vector (EV) transformed poplar and panel (b) shows poplar lines transformed with the cytosolic and lipid droplet (“LD”) co-production vector pWL1HFS2 compared to the same EV samples from panel (a). Leaf samples were taken at random across six leaves for the “F” lines and three leaves for the “E” and “G” lines. Bars represent the mean squalene yield, with dots representing individual measured leaf samples and error bars representing standard error.

While successful transformants producing squalene were generated for the plastidial squalene pathway, it appears that either the overproduction of cytosolic squalene, lipid droplets, or both may be toxic to regenerating poplar plants, though we were unable to confirm this before the plantlets died. When shoots were regenerated from callus, they would often not survive when transferred to rooting medium, suggesting there may be a root specific regeneration issue when these pathways are expressed. Further analysis of young, green stems and root tissue of plastidial squalene lines confirm production is occurring throughout the plants, though with significantly lower yields than leaves (Figure 4c and 4d). It can only be hypothesized why the lipid droplet and squalene co-production pathways appear toxic to the plants. Lipid droplet formation was seen transiently expressing *WRI1* and *EYFP-NoLDSP* in poplar NM6 (Figure S1), confirming the functionality of the platform. It has been demonstrated that WRI1 can influence auxin homeostasis (Kong *et al.*, 2017, 2022) and auxin has been shown to have an essential role in formation of adventitious roots in species like poplar (Bannoud and Bellini, 2021). In this case, overexpression of *WRI1* in stems and roots may be disrupting auxin homeostasis and therefore interfering with adventitious root formation, which is essential for micropropagation of poplar.

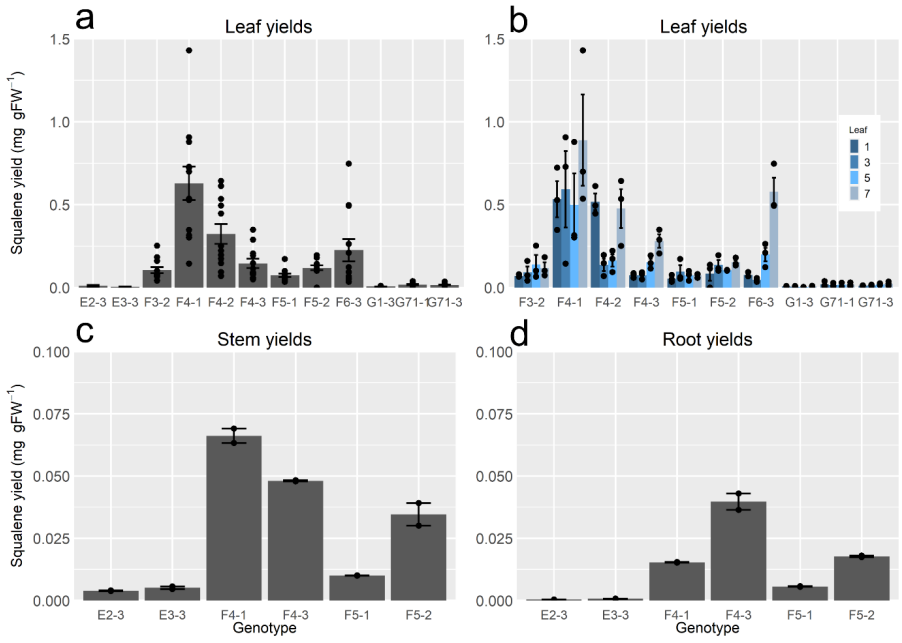

Figure 4: Leaf stage, stem, and root analysis of squalene yields in select poplar transformants. The mean squalene yield (n=12) across four leaf stages (a) and the mean yield (n=3) at each of these four stages (b) was measured. Samples were collected from the first fully expanded leaf (leaf 1), third, fifth, and seventh leaves from three separate branches, representing three biological replicates, with the mean squalene yield for each stage shown in (b) and the mean squalene yield for all 12 samples in (a). Analysis of squalene yields (n=2) in young stems (c), and in roots (d). Empty vector lines E2-3 and E3-3 in panel (a) represent the same data from Figure 5. Each stem and root mean were calculated from two replicates of separate extractions from the same bulk tissue. Dots represent individual measurements and error bars represent standard error.

Previous transient expression experiments in *N. benthamiana* demonstrated squalene yields using lipid droplet scaffolding were more than twice that of the plastidial squalene pathway (Bibik *et al.*, 2022). These results suggest significant increases in transgenic poplar NM6 may be possible through implementation of lipid droplet scaffolding strategies. Future work could incorporate tissue specific expression of lipid droplet and squalene co-production pathways to avoid negative impacts on plant regeneration and development. For example, using leaf specific promoters for each gene in the pathway to reduce possible toxic effects from squalene and lipid droplet co-production in other tissues.

Analysis of isoprene emission and photosynthesis

Previous studies have demonstrated that engineering squalene production in plants can influence photosynthesis (Bibik *et al.*, 2022; Wu *et al.*, 2012; Zhao *et al.*, 2018). Therefore, we sought to determine how these engineered squalene pathways influenced photosynthesis in the transgenic poplar lines. Additionally, with poplar known to emit large amounts of isoprene natively, we aimed to measure how introducing direct competition for IDP/DMADP by the engineered squalene pathway influences total isoprene emission. Three clones of F4 (F4-1, F4-2, and F4-3), two clones of F5 (F5-1 and F5-2), and two independent empty vector lines (E2-3 and E3-3) were chosen to measure changes in isoprene emission and photosynthesis, and how these correlated with differences in squalene yields (Figure 5 and S2). Compared to the empty vector lines, the five squalene producing plants reduced isoprene emission, suggesting squalene production is directly competing with isoprene production in plastids (Figure 5b and S2b). Moreover, reductions in photosynthesis (the rate of CO_2 assimilation) were seen in lines engineered for squalene production (Figure 5c and S2c), consistent with previous studies in different tobacco species (Bibik *et al.*, 2022; Wu *et al.*, 2012).

Deleted: the

Deleted: Also seen were

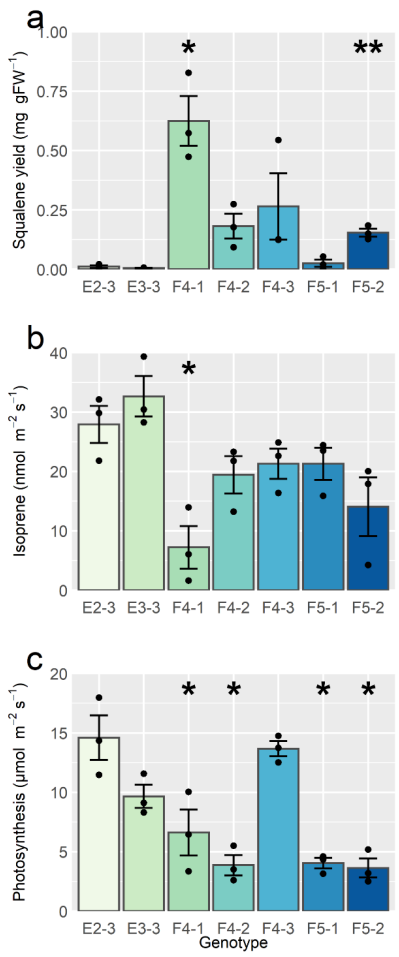

Figure 5: Analysis of isoprene emissions and photosynthesis in squalene producing poplar lines. Five plastid squalene producing transformants, three F4 and two F5 clones, and two empty vector lines, E2-3 and E3-3, were chosen to investigate how squalene production (a) may be affecting isoprene emission rates (b) and photosynthesis (rate of CO_2 assimilation) (c). For each plant the seventh fully formed leaf was selected from three branches to measure isoprene emission and photosynthesis with biological

triplicates. Following measurements, these leaves were collected for squalene extraction. The bars are the mean values (n=3), each dot represents individual measurements, and error bars represent the standard error. Asterisks indicate statistical significance compared to E2-3 ('*': $P < 0.05$; '**': $P < 0.01$) as determined by Student's *t* test.

Isoprene emission in poplar has been implicated to have roles in various biotic and abiotic stresses (Pollastri *et al.*, 2021; Schnitzler *et al.*, 2010), in particular tolerance to heat(Behnke *et al.*, 2007). However, studies have shown non-emitting poplars demonstrate similar biomass productivity to isoprene emitting lines under more temperate conditions (Behnke *et al.*, 2012; Monson *et al.*, 2020). In particular, transgenic lines with suppressed isoprene emission through RNA interference to reduce *ISPS* expression maintained similarly high biomass productivity in a 4-year field trial (Monson *et al.*, 2020). Additionally, this study found increases in expression of compensatory pathways of protective compounds may have enabled this high productivity. This suggests poplar may be amenable to further engineering of plastid terpenoid pathways to redirect IDP/DMADP away from isoprene and towards squalene and other terpenoids with industrial applications. Furthermore, future engineering could incorporate the plastid targeted membrane scaffolding strategies previously developed (Bibik *et al.*, 2022; Zhao *et al.*, 2018), potentially reducing the negative effects plastid squalene production has on photosynthesis.

Technoeconomic analysis of poplar NM6 squalene production

A technoeconomic analysis (TEA) was performed to estimate a minimum selling price (MSP) for squalene produced from the engineered poplar NM6 and, importantly, identify the major economic drivers. Towards this goal, we synthesized a system for the production and recovery of squalene and developed a process simulation model based on a squalene yield of 0.63 mg/gFW, a solvent-to-biomass ratio of 1.092, and a hexane loss of 30% obtained from the lab-scale bulk tissue extractions. Under this base scenario, the resulting MSP is $751/kg, an order of magnitude higher than the current median cost of plant-derived squalene of $40/kg or shark-derived squalene of $45.75/kg (Macdonald and Soll, 2020). The two major cost contributors are the costs of solvent and feedstock, accounting for 87% and 12% of the total cost, respectively (Figure 6a).

Deleted: e measured

Deleted: p

Deleted: p

Formatted: Font: Italic, Complex Script Font: Italic

Formatted: Font: Italic, Complex Script Font: Italic

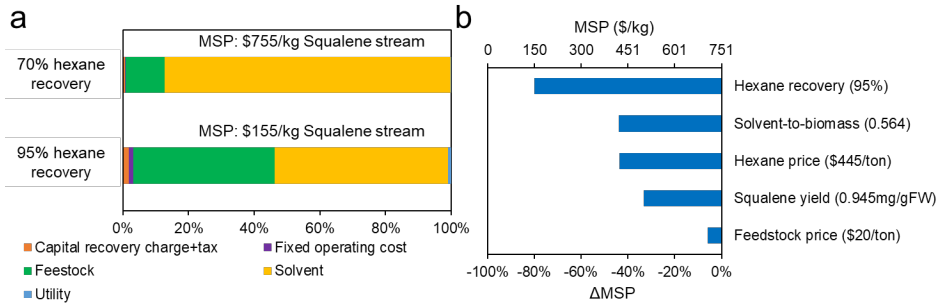

Figure 6: Technoeconomic analysis of squalene production, extraction, and purification from poplar leaves. Panel (a) shows MSPs and cost distributions from technoeconomic analysis with either 70% hexane recovery as measured in the lab simulation or 95% hexane recovery. Panel (b) shows MSP reduction (ΔMSP) from the base case MSP ($751/kg) through the sensitivity analysis of design and cost parameters.

Commented [HB3]: Correction needed: legend, 'feedstock' and alignment of the figures at the top.

A single-point sensitivity analysis was performed to investigate the effects of the parameters related to the two major cost contributors on the process economics. Figure 6b shows reductions in the MSP compared to the base case MSP when (1) increasing the hexane recovery to 95%, (2) decreasing the hexane price by 50%, (3) reducing the solvent-to-biomass ratio by 50%, (4) improving the squalene yield by 50%, and (5) decreasing the feedstock price by 50%. Improving the hexane recovery would significantly decrease the MSP by 80%, to $151/kg (Figure 6a), which is still 3.8 times higher than current plant-derived sources (40/kg). This could be achieved by reducing solvent and feedstock costs, currently accounting for 53% and 43% of the total cost, respectively (Figure 6a). An increase in the hexane recovery would also reduce the required feedstock because of the lower loss of the extracted squalene. Exploring other common industrial extraction processes using hexane or other solvents, like decanter centrifuges, filtration techniques, or solvent evaporation, may allow a much higher hexane recovery (85-95%) (Burke *et al.*, 2011; Lapkin *et al.*, 2006; Sievers *et al.*, 2015; Wikandari *et al.*, 2015). A 50% increase in the squalene yield decreases feedstock and solvent costs and thereby the MSP by 33%. The hexane price could also significantly impact the MSP, whereas the feedstock price has a relatively smaller impact (Figure 6b). Decreasing the solvent-to-biomass ratio could also have a significant impact resulting from decreases in capital, utility, and solvent costs. Accordingly, further research could be aimed at (1)

improving the squalene yield through crop engineering, (2) increasing the solvent recovery, and (3) exploring other candidate solvents that have low price and/or require low solvent-to-biomass ratio. Furthermore, the process we synthesized does not include microbial production from converted lignocellulosic biomass as was performed with sorghum (Yang *et al.*, 2020), which could provide further insight into how terpenoid producing poplar may improve economics of the platform.

Conclusions

In this work, we engineered poplar for production of squalene, which may provide an alternative, sustainable source. Transgenic lines produced up to a mean of 0.63 mg/gFW across leaf stages and accumulated much smaller amounts in stems and roots. While the TEA results indicate that further optimization is needed to improve economic viability, there is great opportunity to further engineer squalene production. To improve plastid targeted squalene production, one strategy which may greatly improve yields would be knockdown or knockout or ISPS to direct more IDP/DMADP towards squalene. As we have previously demonstrated in transient expression systems (Bibik *et al.*, 2022), the cytosolic lipid droplet scaffolding strategy produced more than twice the amount of squalene compared to the plastidial pathway. Here, transgenic poplar lines could not be generated containing this pathway which may be due to constitutive expression of genes interfering with adventitious root formation. Future engineering strategies could incorporate tissue-specific expression of desired pathways to avoid any possible unintended effects in other tissues or during regeneration. This work demonstrates novel engineering approaches in a bioenergy feedstock crop, laying the groundwork for a sustainable terpenoid production platform for and as a potential strategy to improve economic viability of such crops.

Methods

Generation of poplar transformants

Constructs for transformation were derived from the pEAQ-*HT* vector (Peyret and Lomonossoff, 2013) with the P19 gene removed and replaced with a second multiple cloning site (MCS2) (Figure 2). To remove the P19 gene, primers were designed to amplify the entire vector using Phusion® High-Fidelity DNA Polymerase (New England Biolabs), without the P19 gene, and containing 5' overhangs for re-ligating the vector with a SwaI restriction site in place of the gene using In-Fusion cloning mix (Takara

Bio). Therefore, both cloning sites were under the control of the constitutively expressing CaMV 35S promoter.

Each gene was either cloned from cDNA of the native organism or synthesized by Integrated DNA Technologies as gene fragments, similar to previous work (Bibik *et al.*, 2022). All genes used the native DNA sequence except for *MaSQS CΔ17*, which was codon optimized for *Nicotiana benthamiana*, and the LP4/2A linker sequences. There are two DNA sequence variants of LP4/2A linkers to avoid identical sequences and assist with cloning. All sequences were confirmed by Sanger sequencing through Psomagen, Inc., formerly Macrogen Corp. Each set of genes and LP4/2A linkers were consecutively inserted into the indicated MCS (Figure 2) using In-Fusion cloning. To insert genes into MCS1, the vector was first digested by NruI and XhoI restriction enzymes. After confirming insertion of genes into MCS1, the vectors requiring insertion of additional genes into MCS2 were digested by SwaI restriction enzyme prior to insertion of the additional genes.

Poplar P39 transformation attempts were performed similar to methods previously described (Unda *et al.*, 2017). A cork bore was used to remove leaf discs from 4-week-old plantlets grown in tissue culture. Leaf discs were co-incubated with *Agrobacterium tumefaciens* strain C58 (OD_{600} of 0.1-0.2) harboring the appropriate vector at 28°C for 30 min before then being blotted dry and transferred to woody plant medium (WPM) plates containing 0.1 µM of 1-Naphthaleneacetic acid, 6-Benzylaminopurine, and Thidiazuron for 3 days in the dark. Leaf discs were then transferred to WPM plates with 500 µg/mL of carbenicillin and 250 µg/mL cefotaxime, placed in the dark for another 3 days, and replated again to WPM with the same antibiotics with an additional 25 µg/mL of kanamycin for selection of transformants. These plates were kept in low light to allow for shoot regeneration, however, any shoots that formed were unable to develop roots or survive.

The transgenic NM6 poplars were generated as described previously (Han *et al.*, 2013; Ko *et al.*, 2012). Briefly, sterile stem internodes or leaves (1 cm long) taken from *in vitro* grown hybrid poplar NM6 were inoculated with *A. tumefaciens* strain C58 carrying the selected vector construct. Shoot regeneration was induced in the presence of kanamycin. The regenerated shoots were further screened for antibiotic resistance by transferring to rooting media containing kanamycin. An initial round of genomic PCR specific to the selection marker was used to confirm the transgenic events prior to transfer of plantlets to soil. Following rooting and selection marker confirmation, transgenic poplar plantlets were transferred to soil and placed in a growth chamber for acclimation. Chamber conditions were set to a light intensity of 200 µmol m^{-2} s^{-1} at pot level, 12 h day length, 23°C during the day and 20°C during

Deleted: r

the night, and a relative humidity of 60%. Poplar plantlets were allowed to acclimate in the chamber for 2-3 weeks before transplanting to larger pots and transferring to the greenhouse.

The left and right borders of the transfer DNA region were confirmed through isolation of genomic DNA and followed by PCR with two sets of primers specific for regions near the right (forward sequence: 5'-ACGACGGCCAGTGAATTGTT-3', reverse sequence: 5'- GGTTTTGATAAAAGCGAACGTGGG-3') or left (forward sequence: 5'- CATTCGACCACCAAGCGAAACA-3', reverse sequence: 5'-TCTTCTGAGCGGGACTCTGG-3') borders of the transfer DNA region (Figure S4). The genomic DNA was isolated from the first fully formed leaves of each transgenic plant using a 2x CTAB buffer (2% (w/v) cetyltrimethylammonium bromide, 100 mM tris-HCl (pH 8.0), 200 mM ethylenediaminetetraacetic acid (EDTA), 1.4 M NaCl, and 0.2% β-mercaptoethanol). The leaf tissue was frozen and ground to a powder, 500 µL of 2x CTAB added, and incubated at 65°C for 30 min. 500 µL of chloroform was added and the samples vortexed to thoroughly mix. The samples were centrifuged at 17,000 x g for 5 min and 200 µL of the top organic layer transferred to a clean tube. To this organic layer 20 µL of 3 M sodium acetate (pH 5.2) and 400 µL of isopropanol were added prior to mixing by inversion 3 – 5 times. The tubes were then centrifuged at 17,000 x g for 10 min, supernatant poured out, washed with 700 µL of 70% ethanol, and centrifuged again for 5 min. The supernatant was removed, pellet was allowed to dry for 30 min, and finally resuspended in 200 µL of sterile, de-ionized water for analysis.

Transient expression in poplar NM6

Agrobacterium-mediated transient expression was performed similar to methods commonly used in *Nicotiana benthamiana* (Bibik *et al.*, 2022), but in poplar NM6 leaves. *A. tumefaciens* LBA4404 strains harboring a pEAQ-*HT* vector (Peyret and Lomonossoff, 2013; Sainsbury *et al.*, 2009) containing either an *EYFP-NoLDSP* fusion or *AtWI1*-LP4/2A-*EYFP-NoLDSP* were infiltrated with a syringe at an OD_{600} of 1.0. Infiltration was much more difficult than tobacco leaves, however, enough *Agrobacterium* was infiltrated around the infiltration site to measure fluorescence (Figure S1). Infiltrated leaf areas were cut off and using a dulled razor blade the adaxial layers of leaf tissue were gently scraped off to reveal a thin abaxial layer for imaging in an Olympus Fluoview FV10i microscope.

Analysis of squalene production in transformants

Leaf tissue was collected, extracted, and measured using gas chromatography with flame ionization detection similar to methods previously described (Bibik *et al.*, 2022). 23 mm leaf discs were cut, weighed, frozen in liquid nitrogen in 2 mL screw cap tubes containing 0.1 mm glass beads and two 3

mm tungsten carbide beads, and stored at -80°C until extraction. Frozen tissues were ground twice in a Qiagen TissueLyser at 30 m s^{-1} for 2 min, until the tissue was a fine powder. 600µL of hexane containing 50 ng/µL of n-hexacosane was added and samples shaken at room temperature for two hours, 300 µL of water added to aid in separation, and samples were centrifuged at 17,000 x g for 5 mins before transferring the hexane layer to GC vials for analysis. Samples for stem and root extraction were collected from multiple young, green stems or roots, flash frozen in liquid nitrogen and stored at -80°C until extraction. Stem or root samples were ground with a mortar and pestle into a fine powder, approximately 500 mg of ground tissue weighed in 2 mL screw cap tubes, and squalene extracted as described above. Squalene was quantified as previously described (Bibik *et al.*, 2022) by analyzing with gas chromatography with flame ionization detection and comparing peak areas to a calibration curve of known squalene concentrations.

Analysis of isoprene emission and photosynthesis

Isoprene measurements were recorded in real time using a Fast Isoprene Sensor or FIS (Hills Scientific, Boulder, Colorado). Isoprene reacts with ozone to produce formaldehyde and glyoxal that are electronically excited. When they return to the ground state, green light is emitted and photons are detected by a photomultiplier tube (Guenther and Hills, 1998). We measured isoprene emission and photosynthesis rates simultaneously using the FIS and the LI-6800 portable gas exchange system (LI-COR Biosciences, Lincoln, NE) respectively. The airflow from the LI-6800 leaf chamber was redirected to the FIS for isoprene measurement. The flow rate in the LI-6800 was set at 500 µmol s^{-1} and the FIS flow rate was set such that it draws sample air from the LI-6800 at 600 sccm (420 µmol s^{-1}). A 3.225 ppm isoprene standard from Airgas was used for the FIS calibration. First, we determined the background signal by measuring isoprene levels in the air flowing from the gas chamber. Then the leaf was inserted into the chamber and allowed to equilibrate under the following conditions: 1000 µmol m^{-2} s^{-1} light intensity (50% blue light and 50% red light), 30°C, 420 µmol mol^{-1} CO_2 and water vapor content of 22 mmol mol^{-1}. A measurement was logged after both photosynthesis and isoprene reached steady state at the end of the equilibration period. We subtracted the background signal from each reading of isoprene measurement and calculated mean isoprene emission. Photosynthesis was reported by calculating mean of CO_2 assimilation rates recorded for 1 min after stabilization. Measurements were done in three leaves for each genotype. At the end of the day following isoprene emission and photosynthesis measurements, two 23 mm leaf discs were collected, weighed, extracted, and measured as described above.

Deleted: light intensity of

Deleted: temperature of

Deleted: [CO_2] of

Formatted: Subscript

Deleted: over the time period it stabilized

Technoeconomic analysis of squalene producing poplar

The analysis presented was based on a lab-scale extraction of squalene from poplar leaf tissue. Fresh leaf tissue from transgenic poplar line F4-1 was flash frozen in liquid N_2 then ground to a fine powder. Approximately 3 g of ground tissue was weighed in a 50 mL polypropylene conical tube, 5 mL of hexane containing 50 ng/µL of internal standard of n-hexacosane added, samples mixed and allowed to incubate with shaking at room temperature for 2 hr. Tubes were centrifuged at 10,000 x g for 5 mins and as much of the solvent layer as possible was removed with Hamilton syringes to accurately determine the volume of hexane remaining in the leaf tissue layer and unable to be recovered. This extraction resulted in ~70% hexane recovery, which was the value used for the simulation, along with a squalene yield of 0.63 mg/gFW as previously experimentally determined (Figure 3).

Based on the experimental data, an integrated process was designed, and a process simulation model was developed in Aspen Plus. The designed process was composed of (1) extraction of squalene from poplar leaves, (2) separation of solvent phase from aqueous phase, (3) recovery of solvent, and (4) purification of squalene. A detailed process flow diagram is depicted in Figure S3; mass flow rates and energy requirements are provided in Table S1 and Table S2, respectively; capital and operating costs are summarized in Table S3; and economic parameters and assumptions are listed in Table S4. Equipment installed costs and variable operating costs were estimated based on the simulation results at a product flow rate of 100 kg/h. All equipment costs were estimated using an exponential scaling expression(Woods, 2007). A discounted cash flow analysis was performed to calculate the MSP required to obtain a net present value of zero for a given internal rate of return.

Deleted: designed

Accession numbers

AtFDPS:NM_117823.4; *AtWRI1*$^{1\text{-}397}$:AY254038.2; *CfDXS*:KP889115.1; *ElHMGR*$^{159\text{-}582}$:JQ694150.1; *MaSQS CΔ17*:KT318395.1; *NoLDSP*:JQ268559.1

Author contributions and acknowledgements

JDB and BRH conceived the study. JDB wrote the manuscript with contributions from AS for isoprene and photosynthesis measurement methods and BK for technoeconomic analysis results and methods. Pathways and constructs were designed by JDB. Poplar P39 transformation attempts were

performed by JDB and FU, with design and discussion guidance from SDM. Poplar NM6 transformations were performed by the Michigan State University Plant Biotechnology Resource and Outreach Center. Squalene analysis in transgenic lines was performed by JDB. Isoprene emission and photosynthesis experiments were performed by AS and supported by TDS. Squalene analysis from isoprene and photosynthesis studies were performed by JDB and TBA. Technoeconomic analyses were designed by JDB, BRH, BK, and CTM, and performed by BK using data collected by JDB. We would like to thank Malik Sankofa for assistance in maintaining transgenic poplar lines and help with a portion of squalene extractions for data presented in Figure 3. Figures were made using BioRender.com. We collectively acknowledge that Michigan State University occupies the ancestral, traditional, and contemporary Lands of the Anishinaabeg – Three Fires Confederacy of Ojibwe, Odawa, and Potawatomi peoples. In particular, the University resides on Land ceded in the 1819 Treaty of Saginaw. We recognize, support, and advocate for the sovereignty of Michigan's twelve federally-recognized Indian nations, for historic Indigenous communities in Michigan, for Indigenous individuals and communities who live here now, and for those who were forcibly removed from their Homelands. By offering this Land Acknowledgement, we affirm Indigenous sovereignty and will work to hold Michigan State University more accountable to the needs of American Indian and Indigenous peoples.

Funding

This work was supported by the Great Lakes Bioenergy Research Center, U.S. Department of Energy, Office of Science, Office of Biological and Environmental Research under Award Number DE-SC0018409. We would also like to acknowledge partial support from the Department of Biochemistry and Molecular Biology startup funding and support from AgBioResearch (MICL02454).

Data availability

Raw data for figures 3 to 5 is available at Zenodo xxx.

Commented [BH4]: Jake: Please provide data, or point me in the direction. Upload: Bjoern.

Conflict of interest disclosure

The authors declare no conflict of interest.

Short legends for Supporting Information

Figure S1: Transient expression of lipid droplet scaffolding in poplar NM6 leaves.

Figure S2: Additional analysis of isoprene emission and photosynthesis in squalene producing poplar NM6.

Figure S3: Process flow diagram of the simulated squalene extraction and purification from bulk poplar leaves.

Figure S4: Analysis of transgenic poplar gDNA by PCR to confirm T-DNA insertion into the genome of each line.

Table S1: Economic parameters and assumptions used in technoeconomic analyses.

References

An, Y., Liu, Yu, Liu, Yijing, Lu, M., Kang, X., Mansfield, S.D., et al. (2021) *Opportunities and barriers for biofuel and bioenergy production from poplar*. *GCB Bioenergy*, **13**, 905–913.

Bannoud, F. and Bellini, C. (2021) *Adventitious Rooting in Populus Species: Update and Perspectives*. *Front. Plant Sci.*, **12**.

Behnke, K., Ehlting, B., Teuber, M., Bauerfeind, M., Louis, S., Hänsch, R., et al. (2007) *Transgenic, non-isoprene emitting poplars don't like it hot*. *Plant J.*, **51**, 485–499.

Behnke, K., Grote, R., Brüggemann, N., Zimmer, I., Zhou, G., Elobeid, M., et al. (2012) *Isoprene emission-free poplars – a chance to reduce the impact from poplar plantations on the atmosphere*. *New Phytol.*, **194**, 70–82.

Bhalla, A., Bansal, N., Pattathil, S., Li, M., Shen, W., Particka, C.A., et al. (2018) *Engineered Lignin in Poplar Biomass Facilitates Cu-Catalyzed Alkaline-Oxidative Pretreatment*. *ACS Sustain. Chem. Eng.*, **6**, 2932–2941.

Bibik, J.D., Weraduwage, S.M., Banerjee, A., Robertson, K., Espinoza-Corral, R., Sharkey, T.D., et al. (2022) *Pathway Engineering, Re-targeting, and Synthetic Scaffolding Improve the Production of Squalene in Plants*. *ACS Synth. Biol.*

542 Bohlmann, J. and Keeling, C.I. (2008) *Terpenoid biomaterials*. *Plant J.*, **54**, 656–669.

543 Burke, D.R., Anderson, J., Gilcrease, P.C., and Menkhaus, T.J. (2011) *Enhanced solid–liquid clarification of*
544 *lignocellulosic slurries using polyelectrolyte flocculating agents*. *Biomass Bioenergy*, **35**, 391–401.

545 Costa, M.A., Marques, J.V., Dalisay, D.S., Herman, B., Bedgar, D.L., Davin, L.B., and Lewis, N.G. (2013)
546 *Transgenic Hybrid Poplar for Sustainable and Scalable Production of the Commodity/Specialty Chemical,*
547 *2-Phenylethanol*. *PLOS ONE*, **8**, e83169.

548 François, I.E.J.A., Van Hemelrijck, W., Aerts, A.M., Wouters, P.F.J., Proost, P., Broekaert, W.F., and
549 Cammue, B.P.A. (2004) *Processing in* Arabidopsis thaliana *of a heterologous polyprotein resulting in*
550 *differential targeting of the individual plant defensins*. *Plant Sci.*, **166**, 113–121.

551 Grimberg, Å., Carlsson, A.S., Marttila, S., Bhalerao, R., and Hofvander, P. (2015) *Transcriptional*
552 *transitions in* Nicotiana benthamiana *leaves upon induction of oil synthesis by WRINKLED1 homologs*
553 *from diverse species and tissues*. *BMC Plant Biol.*, **15**, 192.

554 Guenther, A.B. and Hills, A.J. (1998) *Eddy covariance measurement of isoprene fluxes*. *J. Geophys. Res.*
555 *Atmospheres*, **103**, 13145–13152.

556 Han, X., Ma, S., Kong, X., Takano, T., and Liu, S. (2013) *Efficient Agrobacterium-Mediated Transformation*
557 *of Hybrid Poplar* Populus davidiana *Dode ×* Populus bollena *Lauche*. *Int. J. Mol. Sci.*, **14**, 2515–2528.

558 Ko, J.-H., Kim, H.-T., Hwang, I., and Han, K.-H. (2012) *Tissue-type-specific transcriptome analysis identifies*
559 *developing xylem-specific promoters in poplar*. *Plant Biotechnol. J.*, **10**, 587–596.

560 Kong, Q., Low, P.M., Lim, A.R.Q., Yang, Y., Yuan, L., and Ma, W. (2022) *Functional Antagonism of WRI1*
561 *and TCP20 Modulates GH3.3 Expression to Maintain Auxin Homeostasis in Roots*. *Plants*, **11**, 454.

562 Kong, Q., Ma, W., Yang, H., Ma, G., Mantyla, J.J., and Benning, C. (2017) *The* Arabidopsis *WRINKLED1*
563 *transcription factor affects auxin homeostasis in roots*. *J. Exp. Bot.*, **68**, 4627–4634.

564 Labrecque, M. and Teodorescu, T.I. (2005) *Field performance and biomass production of 12 willow and*
565 *poplar clones in short-rotation coppice in southern Quebec (Canada)*. *Biomass Bioenergy*, **29**, 1–9.

566 Lapkin, A.A., Plucinski, P.K., and Cutler, M. (2006) *Comparative Assessment of Technologies for*
567 *Extraction of Artemisinin*. *J. Nat. Prod.*, **69**, 1653–1664.

Lee, D.W., Lee, S., Lee, G., Lee, K.H., Kim, S., Cheong, G.-W., and Hwang, I. (2006) *Functional Characterization of Sequence Motifs in the Transit Peptide of* Arabidopsis *Small Subunit of Rubisco*. *Plant Physiol.*, **140**, 466–483.

Lu, D., Yuan, X., Kim, S.-J., Marques, J.V., Chakravarthy, P.P., Moinuddin, S.G.A., et al. (2017) *Eugenol specialty chemical production in transgenic poplar (*Populus tremula × P. alba*) field trials*. *Plant Biotechnol. J.*, **15**, 970–981.

Ma, W., Kong, Q., Grix, M., Mantyla, J.J., Yang, Y., Benning, C., and Ohlrogge, J.B. (2015) *Deletion of a C–terminal intrinsically disordered region of WRINKLED1 affects its stability and enhances oil accumulation in* Arabidopsis. *Plant J.*, **83**, 864–874.

Macdonald, C. and Soll, J. (2020) *Shark conservation risks associated with the use of shark liver oil in SARS-CoV-2 vaccine development*. 2020.10.14.338053.

Monson, R.K., Winkler, B., Rosenstiel, T.N., Block, K., Merl-Pham, J., Strauss, S.H., et al. (2020) *High productivity in hybrid-poplar plantations without isoprene emission to the atmosphere*. *Proc. Natl. Acad. Sci.*, **117**, 1596–1605.

Peyret, H. and Lomonossoff, G.P. (2013) *The pEAQ vector series: the easy and quick way to produce recombinant proteins in plants*. *Plant Mol. Biol.*, **83**, 51–58.

Pichersky, E. and Raguso, R.A. (2018) *Why do plants produce so many terpenoid compounds? New Phytol.*, **220**, 692–702.

Pollastri, S., Baccelli, I., and Loreto, F. (2021) *Isoprene: An Antioxidant Itself or a Molecule with Multiple Regulatory Functions in Plants? Antioxidants*, **10**, 684.

Reed, J., Stephenson, M.J., Miettinen, K., Brouwer, B., Leveau, A., Brett, P., et al. (2017) *A translational synthetic biology platform for rapid access to gram-scale quantities of novel drug-like molecules*. *Metab. Eng.*, **42**, 185–193.

Sadre, R., Kuo, P., Chen, J., Yang, Y., Banerjee, A., Benning, C., and Hamberger, B. (2019) *Cytosolic lipid droplets as engineered organelles for production and accumulation of terpenoid biomaterials in leaves*. *Nat. Commun.*, **10**, 853.

Sainsbury, F., Thuenemann, E.C., and Lomonossoff, G.P. (2009) *pEAQ: versatile expression vectors for easy and quick transient expression of heterologous proteins in plants*. *Plant Biotechnol. J.*, **7**, 682–693.

Sannigrahi, P., Ragauskas, A.J., and Tuskan, G.A. (2010) *Poplar as a feedstock for biofuels: A review of compositional characteristics*. *Biofuels Bioprod. Biorefining*, **4**, 209–226.

Schnitzler, J.-P., Louis, S., Behnke, K., and Loivamäki, M. (2010) *Poplar volatiles – biosynthesis, regulation and (eco)physiology of isoprene and stress-induced isoprenoids*. *Plant Biol.*, **12**, 302–316.

Sievers, D.A., Lischeske, J.J., Biddy, M.J., and Stickel, J.J. (2015) *A low-cost solid–liquid separation process for enzymatically hydrolyzed corn stover slurries*. *Bioresour. Technol.*, **187**, 37–42.

Sun, H., Zhou, N., Wang, H., Huang, D., and Lang, Z. (2017) *Processing and targeting of proteins derived from polyprotein with 2A and LP4/2A as peptide linkers in a maize expression system*. *PLOS ONE*, **12**, e0174804.

Unda, F., Kim, H., Hefer, C., Ralph, J., and Mansfield, S.D. (2017) *Altering carbon allocation in hybrid poplar (*Populus alba × grandidentata*) impacts cell wall growth and development*. *Plant Biotechnol. J.*, **15**, 865–878.

Vieler, A., Brubaker, S.B., Vick, B., and Benning, C. (2012) *A Lipid Droplet Protein of* Nannochloropsis *with Functions Partially Analogous to Plant Oleosins*. *Plant Physiol.*, **158**, 1562–1569.

Vining, K., Pomraning, K.R., Wilhelm, L.J., Ma, C., Pellegrini, M., Di, Y., et al. (2013) *Methylome reorganization during in vitro dedifferentiation and regeneration of* Populus trichocarpa. *BMC Plant Biol.*, **13**, 92.

Wikandari, R., Nguyen, H., Millati, R., Niklasson, C., and Taherzadeh, M.J. (2015) *Improvement of Biogas Production from Orange Peel Waste by Leaching of Limonene*. *BioMed Res. Int.*, **2015**, e494182.

Woods, D.R. (2007) *Rules of thumb in engineering practice*. John Wiley & Sons.

Wu, S., Jiang, Z., Kempinski, C., Eric Nybo, S., Husodo, S., Williams, R., and Chappell, J. (2012) *Engineering triterpene metabolism in tobacco*. *Planta*, **236**, 867–877.

Wu, S., Schalk, M., Clark, A., Miles, R.B., Coates, R., and Chappell, J. (2006) *Redirection of cytosolic or plastidic isoprenoid precursors elevates terpene production in plants*. *Nat. Biotechnol.*, **24**, 1441–1447.

Yang, M., Baral, N.R., Simmons, B.A., Mortimer, J.C., Shih, P.M., and Scown, C.D. (2020) *Accumulation of high-value bioproducts in planta can improve the economics of advanced biofuels*. *Proc. Natl. Acad. Sci.*, **117**, 8639–8648.

Yevtushenko, D.P. and Misra, S. (2010) *Efficient* Agrobacterium*-mediated transformation of commercial hybrid poplar* Populus nigra *L. ×* P. maximowiczii *A. Henry*. *Plant Cell Rep.*, **29**, 211–221.

Yuan, L. and Grotewold, E. (2015) *Metabolic engineering to enhance the value of plants as green factories*. *Metab. Eng.*, **27**, 83–91.

Zhang, W., Wang, Y., Diao, S., Zhong, S., Wu, S., Wang, L., et al. (2021) *Assessment of Epigenetic and Phenotypic Variation in* Populus nigra *Regenerated via Sequential Regeneration*. *Front. Plant Sci.*, **12**.

Zhao, C., Kim, Y., Zeng, Y., Li, M., Wang, X., Hu, C., et al. (2018) *Co-Compartmentation of Terpene Biosynthesis and Storage via Synthetic Droplet*. *ACS Synth. Biol.*, **7**, 774–781.

Zhou, S., Runge, T., Karlen, S.D., Ralph, J., Gonzales-Vigil, E., and Mansfield, S.D. (2017) *Chemical Pulping Advantages of Zip-lignin Hybrid Poplar*. *ChemSusChem*, **10**, 3565–3573.

Tables

Figure legends

Figures

Abbreviations

DMADP – Dimethylallyl diphosphate

DXS – 1-deoxy-d-xylulose-5-phosphate synthase

FDP – Farnesyl diphosphate

FDPS – Farnesyl diphosphate synthase

gFW – Grams fresh weight

HMGR – 3-hydroxy-3-methylglutaryl-CoA reductase

IDP – Isopentenyl diphosphate

ISPS – Isoprene synthase

LDSP – Lipid Droplet Surface Protein

MCS – Multiple cloning site

MEP – Methylerythritol 4-phosphate pathway

MSP – Minimum selling price

MVA – Mevalonate pathway

SQS – Squalene synthase

TEA – Technoeconomic analysis

WPM – Woody plant medium

WRI1 – Wrinkled1